ambience is crucial to process reproducibility and reliability.

Acknowledgments

Useful discussions with F. M. d'Heurle are acknowledged with pleasure. The authors would like to thank the Yorktown Silicon Facility, especially S. Brodsky for processing of the films, P. Saunders for the RBS data and R. Savoy for the x-ray microprobe data, and T. Ross for the electron micrographs.

Manuscript submitted March 4, 1985; revised manuscript received June 10, 1985. This was Paper 56 presented at the Cincinnati, Ohio, Meeting of the Society, May 6-11, 1984.

IBM Corporation assisted in meeting the publication costs of this article.

REFERENCES

1. C. M. Osburn, M. Y. Tsai, S. Roberts, C. J. Lucchese, and C. Y. Ting, in "VLSI Science and Technology," C. J. Dell'Oca and W. M. Bullis, Editors, p. 213, The Electrochemical Society Softbound Proceedings Series, Pennington, NJ (1982).
2. C. Y. Ting, S. S. Iyer, C. M. Osburn, G. J. Hu, and A. M. Schweighart, in "VLSI Science and Technology," C. J. Dell'Oca and W. M. Bullis, Editors, p. 224, The Electrochemical Society Softbound Proceedings Series, Pennington, NJ (1982).
3. C. K. Lau, Y. C. Lee, D. B. Scott, J. M. Bridges, J. M. Perma, and R. D. Davies, *IEDM Tech. Dig.*, 714 (1982).
4. H. K. Park, J. Sachitano, G. Eiden, E. Lane, and T. Yamaguchi, *J. Vac. Sci. Technol. A*, **2,** 259 (1984).
5. R. W. Bower and J. W. Mayer, *Appl. Phys. Lett.*, **20,** 369 (1972).
6. W. K. Chu, S. S. Lau, J. Mayer, H. Muller, and K. N. Tu, *Thin Solid Films*, **25,** 393 (1975).
7. L. S. Hung, J. Gyulai, J. W. Mayer, S. S. Lau, and M-A. Nicolet, *J. Appl. Phys.*, **54,** 5076 (1983).
8. R. W. Bene and M. Y. Yang, *J. Electron. Mater.*, **12,** 1 (1983).
9. H. Kato and Y. Nakamura, *Thin Solid Films*, **34,** 135 (1976).
10. R. Butz, G. W. Rubloff, T. Y. Tan, and P. S. Ho, *Phys. Rev. B*, **30,** 5421 (1984).
11. C. Y. Ting, M. Wittmer, S. S. Iyer, and S. Brodsky, in "VLSI Science and Technology/1984," K. E. Bean and G. A. Rozgonyi, Editors, p. 397, The Electrochemical Society Softbound Proceedings Series, Pennington, NJ (1984).
12. A. R. Miedema, *Solid-State Commun.*, **39,** 1337 (1981).
13. H. Condrad, *Prog. Mater. Sci.*, **26,** 131 (1981).
14. M. Berti, A. V. Drigo, C. Cohen, J. Siejka, G. G. Bentini, R. Nipoti, and S. Guerri, *J. Appl. Phys.*, **55,** 3558 (1984).
15. C. Y. Ting, Unpublished data.
16. F. M. d'Heurle, Submitted to *J. Appl. Phys.*

Properties of Tungsten Film Deposited on GaAs by RF Magnetron Sputtering

Nobuhiko Susa, Seigo Ando, and Sadao Adachi

Nippon Telegraph and Telephone Corporation, Musashino Electrical Communication Laboratory, Musashino-shi, Tokyo 180, Japan

ABSTRACT

The crystalline and electrical properties of W films are studied with regard to their relation to Ar sputtering pressure. An α-W phase is formed at a pressure below 5×10^{-2} torr, and its density is 19.2 g/cm^3, independent of the pressure. Above 5×10^{-2} torr, the β-W phase and WO_3 are detected by x-ray diffraction, and the oxygen and carbon are detected by SIMS. The RIE etching rate is found to be independent of the pressure for the α-W phase. This rate increases with Ar pressure after β-W phase formation, and the etching characteristic suffers from aging after deposition. Resistivity is found to be related to density rather than grain size. The W-GaAs Schottky characteristics are somewhat influenced by the pressure. Degradation in carrier density, barrier height, and dark current caused by sputtering damage can be recovered by annealing.

Refractory metals such as tungsten are attractive for use as interconnections in VLSI's because of their low resistivity and fine patternability (1-4). Recently, W films have also been used as bases embedded in a GaAs epitaxial layer, thus facilitating the fabrication of GaAs permeable base transistors (PBT) (5, 6). In these papers, no changes in W Schottky characteristics were observed at MO-CVD growth temperatures of 600°-800°C (7). Although W films have received much attention as interconnections for LSI's, only a few studies have been carried out on their electrical properties when applied as Schottky contacts deposited on GaAs (8, 9).

Tungsten films have been fabricated by CVD (10, 11), electron-beam evaporation (12), and sputtering (13, 14). The properties of W films deposited by sputtering are known to depend on the sputtering pressure. In the present experiment, the crystalline and electrical properties of W films prepared by RF magnetron sputtering were studied, especially the characteristics of W Schottky contacts. The observed characteristics were then analyzed in terms of their relations to the Ar sputtering pressure.

Film Deposition and Crystalline Properties

Film deposition.—The W films were prepared by RF magnetron sputtering (ULVAC, SBR-1304E) at an Ar pressure ranging from 1×10^{-2} to 2×10^{-1} torr. Prior to Ar gas introduction, the chamber was evacuated on the order of 10^{-7} torr with a He cryogenic pump. The W target was cleaned by presputtering for 30 min at 200W. During deposition, the RF power was set at 50W. The substrate bias was 0 V, and no substrate was intentionally heated.

At a 50W input, however, the substrate temperature increased to about 100°C during the deposition. Film thicknesses were measured with a mechanical stylus. The W films on the substrates were partially lifted off by photolithography in order to measure the thickness. Film thicknesses were in the range of 500-6000Å.

The deposition rate increased with Ar pressure, as shown in Fig. 1a. When the Ar pressure exceeded 1×10^{-1} torr, the deposition rate increased sharply. This is primarily due to the increase in the ion flux rather than the reduction in density, because the films deposited above 1×10^{-1} torr were heavier than those prepared at low pressures for an identical deposition time.

It is well known that stress in W films is compressive at low Ar pressures, while being tensile at high pressures (4). Cracks are sometimes observed in thick W films deposited on GaAs substrates due to this stress. The use of thick films, however, is required to control the device characteristics of a PBT, which has a W Schottky electrode embedded in the GaAs as described before. The existence of cracks was examined in relation to Ar pressure

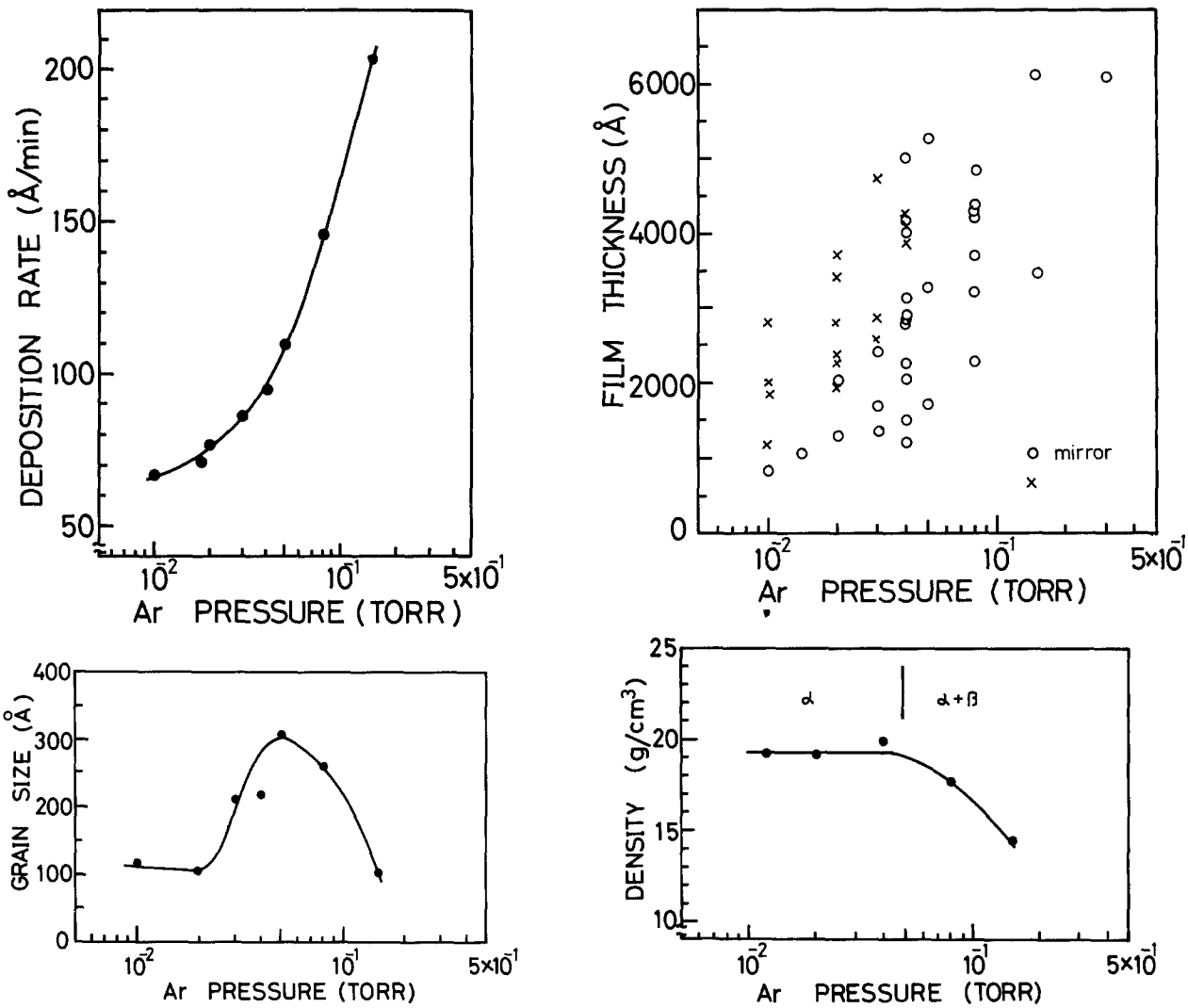

Fig. 1. Deposition rate (a, top left), existence of cracks, (b, top right) density (c, botton left), and grain size (d, bottom right), as functions of sputtering pressure.

and film thickness, and the results are shown in Fig. 1b. Films thicker than 1000Å cannot be obtained at low Ar pressures, while thick films containing no cracks can be deposited at higher pressures.

The reason for this is not clear. The substrate temperature rose to about 100°C, even when the substrate was not intentionally heated. Thermal expansion coefficients are 4.2×10^{-6} and 6.0×10^{-6} °C^{-1} for W (15) and GaAs (16), respectively. Since the temperature of the substrate is cooled from 100°C to room temperature after deposition, compressive stress, caused by the difference in thermal expansion coefficients between W and GaAs, is induced in the W films. The compression initially existing in the W film deposited at a low Ar pressure, due to the peening effect, increases during this cooling period. However, tension in the films prepared at the higher pressure was reduced after deposition. The W films deposited at the lower pressures suffer from larger compressive stress and may contain cracks. The densities of the films deposited at the higher pressures were smaller than those for the lower pressure, as will be described in the following section. Films prepared at higher pressures may be porous and may withstand greater stress than films prepared at the lower pressures.

Density and grain size.—Densities of the W films deposited on glass plates are shown in Fig. 1c as a function of the sputtering pressure. The density was obtained from the weight increase and film volume after W deposition. Densities were 19.2 g/cm³ and were independent of the Ar pressure in the range of $1\text{-}5 \times 10^{-2}$ torr; however, they decreased above this range. The W films were revealed to be in the α-W phase for the Ar pressure of $1\text{-}5 \times 10^{-2}$ torr, while the β-W phase was formed above 5×10^{-2} torr, as shown in Fig. 2.

The smaller density obtained for the high Ar pressure is related to the existence of the β phase rather than the grain size. This is because the W films having the α phase and prepared at $1\text{-}2 \times 10^{-2}$ torr showed a large density of 19.2 g/cm³ even when the grain size was small, as shown in Fig. 1d. However, the existence of the β phase alone cannot explain the lower density, as described below. The α-W phase has a body-centered cubic structure with a 3.16Å lattice constant. The β-W phase structure is an A-15-type structure having a 5.04Å lattice constant, and is body-centered cubic having two atoms on each of its {100} planes (17). Densities calculated from the above parameters for the α and β phases are quite similar: 19.4 and 19.1 g/cm³, respectively. Thus, the presence of the β phase alone cannot cause the lower density.

Since WO_3 has a lower density than that of metal, it is possible that the WO_3, which was always detected by x-ray diffraction for samples consisting mainly of the β-W phase, is responsible for the low density. The larger deposition rate may also cause the low density by making the deposited film porous.

The grain sizes of the W films were determined from x-ray line broadening analysis and are plotted in Fig. 1c. The (110) α phase diffraction patterns were used for analysis. The grain size became small when the β-W phase was formed, as reported in a previous paper (14). Grain size, however, was also small for the films prepared at $1\text{-}2 \times 10^{-2}$ torr, in spite of the presence of the α-W phase. The influence of grain size on resistivity will be discussed later.

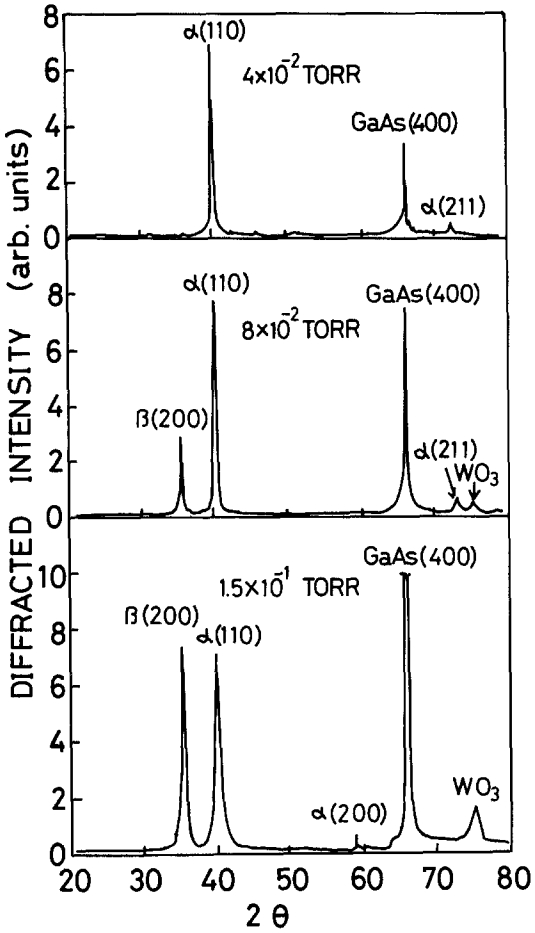

Fig. 2. X-ray diffraction patterns for W films deposited on GaAs at 4 × 10^{-2}, 8 × 10^{-2}, and 1.5 × 10^{-1} torr.

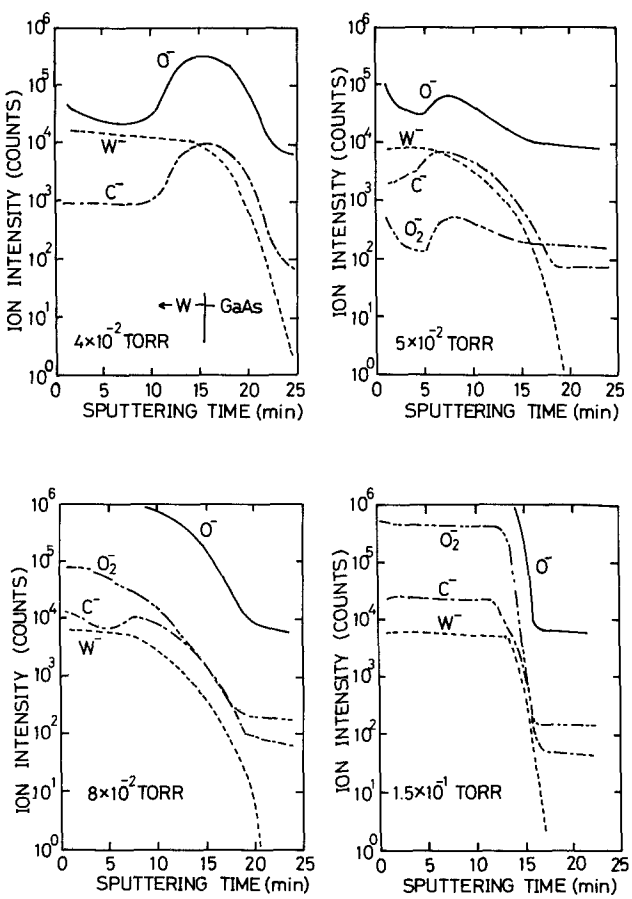

Fig. 3. Impurity profiles measured by SIMS for W films prepared on GaAs at 4 × 10^{-2}, 5 × 10^{-2}, 8 × 10^{-2}, and 1.5 × 10^{-2} torr.

Orientation and impurity. The x-ray diffraction pattern for the W films deposited on GaAs changed when the Ar sputtering pressure was varied, as shown in Fig. 2. Below a 5 × 10^{-2} torr Ar pressure, diffraction from the α(110), α(211) planes was observed. The intensity ratios of α(211) to α(110) x-ray diffractions were 0.08 and 0.2 for the present experiment and for the ASTM data on W powder, respectively. This implies that the films deposited at below 5 × 10^{-2} torr were well oriented in the <110> direction.

The β(200) diffraction was observed for films prepared at above 5 × 10^{-2} torr, and WO_3 diffraction also was observed. The WO_3 was always detected when the β-W phase was formed. These results are consistent with previous reports suggesting that oxygen stabilizes the β phase (12, 13, 18). Etching characteristics, density, grain size, and impurity content changed owing to the existence of the β-W phase, as will be described below.

Impurities in the W films deposited on the GaAs such as oxygen and carbon were analyzed by secondary ion mass spectroscopy (SIMS), and the films were bombarded by a Cs^+ ion beam. The bombarded area was 60 μm in diameter. The results are shown in Fig. 3. The W films with a 2000-6000Å thickness were sputtered by Cs^+ ions. Data on the W-GaAs interface were not very accurate, because the W film surface, sputtered by the Cs^+ ions, became rough during the sputter etching. When the W film was deposited at a high Ar pressure, oxygen and carbon contents increased. In particular, oxygen increased rapidly with an increase in the Ar pressure. The existence of oxygen was also detected by the x-ray diffraction as a part of the WO_3.

At the W-GaAs interface, C and O concentrations were large, as in the case for GaAs epitaxial layers grown on a GaAs substrate. They are probably due to the existence of the GaAs surface oxide layer and also due to C contamination before W deposition.

For the application to device fabrication, the etching rate for reactive ion etching (RIE) using CF_4 was studied with respect to the W deposition pressure dependence. The etching rate for RIE is shown in Fig. 4 as a function of pressure. The W films were etched under the conditions of 50W and 10 Pa (7.5 × 10^{-2} torr). The etching rate was constant for the W films deposited at below 5 × 10^{-2} torr Ar pressure and was independent of time after deposition. On the other hand, the etching rate increased with an increase in the sputtering pressure above 5 × 10^{-2} torr. This etching rate, however, decreased after 2 months. The etching rate increased when the β-W phase was formed and the film density decreased. Although the reason for the reduction in the etching rate after 2 months is not clear, it seems to be related to the existence of the β-W phase.

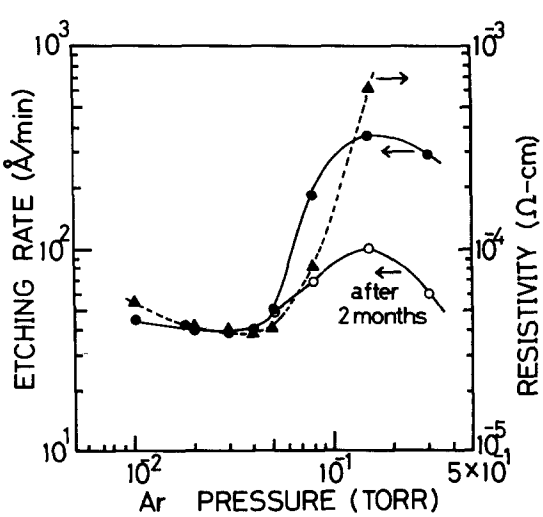

Fig. 4. Etching rates of RIE measured immediately after and 2 months after W deposition and resistivity, as functions of sputtering pressure.

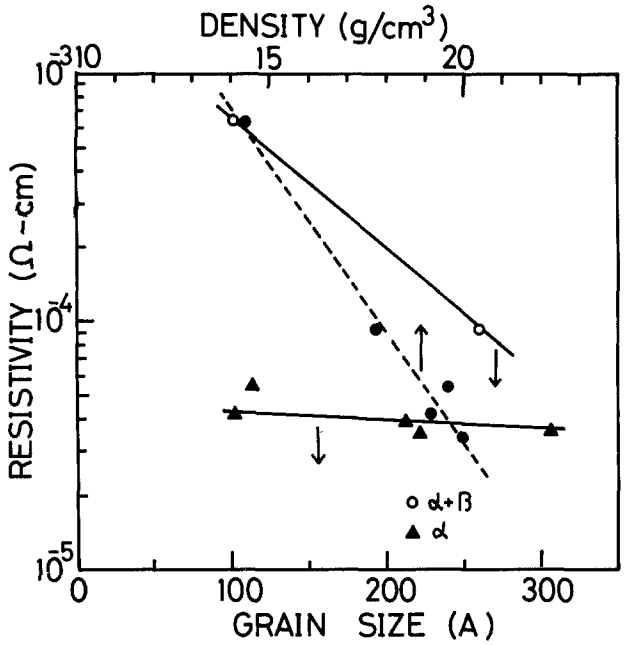

Fig. 5. Resistivity as a function of density and grain size

Electrical Properties

Resistivity.—The resistivity of W films deposited on semi-insulating GaAs is also shown in Fig. 4. A four-point probe was used for the measurement. These results were similar to those for W films prepared on glass plates. The α-W films exhibited lower resistivity than those in the β-W phase (14, 19). Resistivity decreased slightly when the deposition pressure increased in the range of 1-2 $\times$ 10^{-2} torr. This was probably due to the smaller grain size as shown in Fig. 1c.

Resistivity is plotted in Fig. 5 as a function of W film density. It can be seen that resistivity is related to the film density as well as volume fractions of β- and α-W phases.

Figure 5 shows resistivity as a function of grain size calculated from the x-ray diffraction pattern. Data for the α-W phase are somewhat influenced by the grain size, contrary to a previous report (14). The resistivity is 5 $\times$ 10^{-5} Ω-cm when grain size is extrapolated to zero. Since this value is larger by about one order of magnitude than that for the bulk, it is concluded that scattering resulting from impurities and defects is larger than that caused by the grain boundary.

Schottky characteristics.—When the W film is applied to devices such as a PBT, Schottky characteristics are important for realizing good device performance. Tungsten film was deposited on a GaAs epitaxial layer grown on a n^+-GaAs substrate. The epitaxial layer was 2.6 μm thick, and its carrier concentration was 1 $\times$ 10^{17} cm^{-3}. Ohmic contacts (alloyed Au-Ge-Ni) were formed on the n^+-GaAs substrates. A W Schottky contact of 200 μm diam was deposited through metal mask. Ideality factor, n, and barrier height, ϕ_{Bn}, obtained from the forward current and voltage characteristics (20), are shown in Fig. 6. The ideality factor increased from 1.03 to 1.06 when the sputtering pressure was varied from 1 $\times$ 10^{-2} to 2 $\times$ 10^{-1} torr. However, the barrier height was 0.6 eV, and was constant in the range of 1-5 $\times$ 10^{-2} torr, where the α-W phase existed. The barrier height increased to 0.64 eV for a 2 $\times$ 10^{-1} torr Ar pressure.

Leakage currents for diodes were larger at a reverse bias voltage by several orders of magnitude than those for diodes with a Au Schottky contact prepared by Au vacuum evaporation. The carrier concentration profile, calculated from the C-V characteristics, showed that the carrier density decreased at the W-GaAs interface as a result of sputtering damage to the epitaxial layer surface during the deposition. In order to improve the crystal quality, an attempt to anneal GaAs deposited with W film was carried out at 430°C.

Annealing.—The GaAs diodes having W Schottky contacts were annealed at 430°C in a 10% H_2-90% He gas flow.

Carrier concentration profiles obtained from the C-V characteristics are shown in Fig. 7. A sample was annealed for 3 min at 430°C. The carrier density was reduced at the W-GaAs interface by sputtering damage for the as-deposited diodes. After annealing, the reduction in the carrier was recovered by performing a relatively short annealing process.

Dark currents for diodes with as-deposited and annealed (2 min) W contacts as well as a reference (Au Schottky) contact are shown in Fig. 8a as a function of reverse bias voltage. The dark current can be reduced by about one order of magnitude as a result of annealing. However, no further dark current reduction was observed for annealing of over 2 min. The dark currents for annealed diodes, however, were still larger than those for the reference.

Forward currents for diodes with as-sputtered and annealed W contacts are shown in Fig. 8b. The W film was prepared at 4 $\times$ 10^{-2} torr. Data for the diode having the Au evaporated Schottky contact are also shown for reference. The barrier height increased from 0.55 to 0.61 eV owing to annealing. A similar improvement in barrier height has been reported by Sinha (9). The barrier height obtained from the I-V characteristics agreed with that calculated from the C-V characteristics. However, barrier height for as-deposited diodes calculated from the C-V characteristics (0.66 eV) was higher than that obtained from the I-V characteristics (0.55 eV). The values obtained

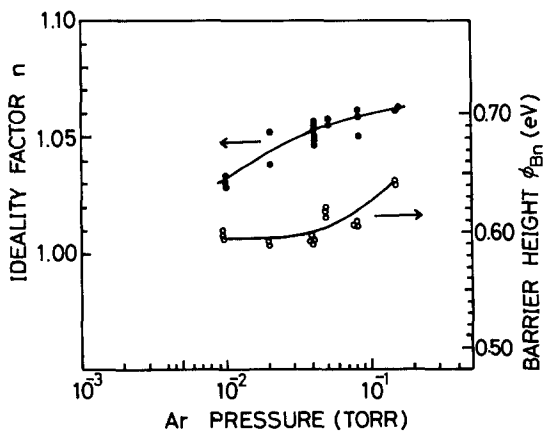

Fig. 6. Ideality factor and barrier height as a function of sputtering pressure.

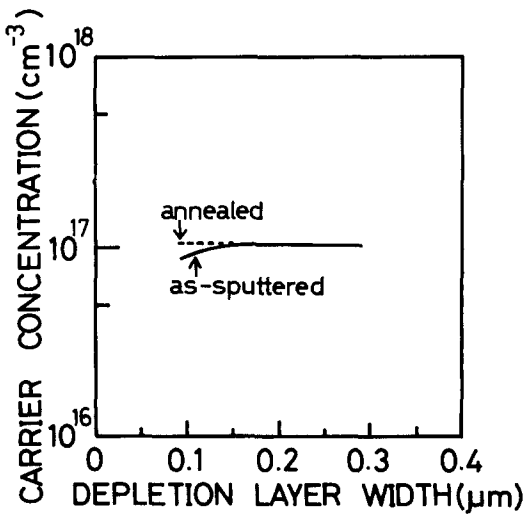

Fig. 7. Carrier concentration profiles for GaAs diodes with as-sputtered and annealed W contacts.

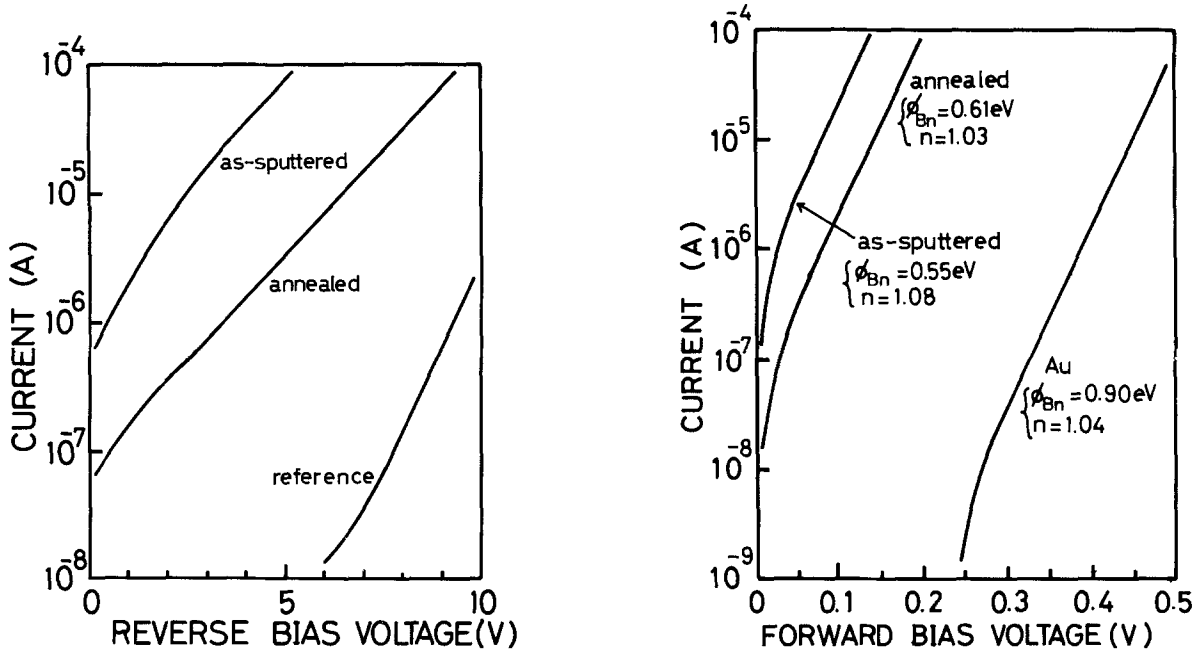

Fig. 8. Reverse (a, left) and forward (b, right) currents for diodes with as-sputtered and annealed W Schottky contacts as functions of bias voltage. Currents for diode having Au evaporated Schottky contact are shown for reference.

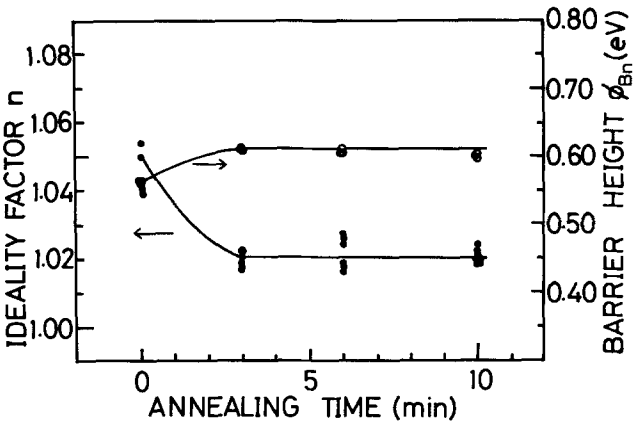

Fig. 9. Ideality factor and barrier height as a function of annealing time.

from the C-V measurement became much larger than those for the C-V characteristics when the damage was seriously increased. This suggests that an insulator layer was formed by sputtering deposition (21).

The ideality factor decreased slightly from 1.08 to 1.04 owing to annealing. No further improvement in the ideality factor or barrier height was observed for a heat-treatment of longer than 3 min, as shown in Fig. 9.

Conclusion

Properties of W films deposited by RF magnetron sputtering were investigated in terms of their relation to Ar sputtering pressure, which ranged from 1×10^{-2} to 3×10^{-1} torr. Below 5×10^{-2} torr, an α-W phase was formed and the density was 19.2 g/cm^3, independent of the Ar pressure. The β-W phase and WO_3 were detected by x-ray diffraction for films prepared at pressures above 5×10^{-2} torr. Oxygen and carbon contained in the W films as impurities increased with the pressure. The RIE etching rate was found to be independent of the pressure for the α-W film. This rate increased with an increase in β-W phase content in W films and was dependent on time after deposition.

Resistivity increased sharply when the volume fractions for the β-W phase and WO_3 were increased. Density rather than grain size was found to affect the resistivity.

The Schottky characteristics of W-GaAs diodes were studied. The barrier height and ideality factor were influenced somewhat by the sputtering pressure. Degradation of barrier height, carrier concentration, as well as the increase in dark current due to sputtering damage, can be recovered by carrying out annealing at 430°C for 2-3 min.

Acknowledgments

The authors would like to express their gratitude to Dr. Kenji Kamabe, Dr. Hideo Sugiura, and Dr. Yoshifumi Takanashi for their helpful discussions. They are also grateful to Hiromitsu Asai for the x-ray diffraction measurements and Yoshikazu Homma for the SIMS measurements.

Manuscript submitted Dec. 27, 1984; revised manuscript received May 22, 1985.

Nippon Telegraph and Telephone Corporation assisted in meeting the publication costs of this article.

REFERENCES

1. P. L. Shah, *IEEE Trans. Electron Devices*, **ed-26,** 631 (1979).
2. A. K. Sinha, *Jpn. J. Appl. Phys.*, Suppl. 2, 487 (1974).
3. S. Iwata, N. Yamamoto, N. Kobayashi, T. Terada, and T. Mizutani, *IEEE Trans. Electron Devices*, **ed-31,** 1174 (1984).
4. R. S. Wagner, A. K. Sinha, T. T. Sheng, H. J. Levinstein, and F. B. Alexander, *J. Vac. Sci. Technol.*, **11,** 582 (1974).
5. C. O. Bozler and G. D. Alley, *IEEE Trans. Electron Devices*, **ed-27,** 1128 (1980).
6. H. Asai, S. Adachi, S. Ando, and K. Oe, *J. Appl. Phys.*, **55,** 3868 (1984).
7. K. Matsumoto, N. Hashizume, H. Tanoue, and T. Kanayama, *Jpn. J. Appl. Phys.*, **21,** L393 (1982).
8. P. M. Batev, M. D. Ivanovitch, E. I. Kafedjiska, and S. S. Simeonov, *Phys. Status Solidi A*, **45,** 671 (1978).
9. A. K. Sinha, *Appl. Phys. Lett.*, **26,** 171 (1975).
10. W. A. Metz, J. E. Mahan, V. Malhotra, and T. L. Martin, *ibid.*, **44,** 1139 (1984).
11. C. M. Melliar-Smith, A. C. Adams, R. H. Kaiser, and R. A. Kushner, *This Journal*, **121,** 298 (1974).
12. B. Basavaiah and S. R. Pollach, *J. Appl. Phys.*, **39,** 5548 (1968).
13. P. M. Petroff and W. A. Reed, *Thin Solid Films*, **21,** 73 (1974).
14. P. Petroff, T. T. Sheng, A. K. Sinha, G. A. Rozgonyi, and F. B. Alexander, *J. Appl. Phys.*, **44,** 2545 (1973).
15. "Metal Handbook," American Society for Metals, Metals Park, OH (1948).
16. M. E. Straumanis and C. D. Kim, *Acta. Crystollogr.*, **19,** 256 (1965).
17. W. R. Morcom, W. L. Worrell, H. G. Sell, and H. I.

Kaplan, *Metall. Trans.*, **5**, 155 (1974).
18. C. C. Tang and D. W. Hess, *Appl. Phys. Lett.*, **45**, 633 (1984).
19. D. W. Hoffman and J. A. Thornton, *Thin Solid Films*, **45**, 387 (1977).
20. S. M. Sze, "Physics of Semiconductor Devices," pp. 279-284, Wiley-Interscience, New York (1981).
21. J. R. Waldrop, *Appl. Phys. Lett.*, **41**, 350 (1982).

An Experimental and Theoretical Study of the Infrared Reflectance of Thin Oxide Films on Metals

David K. Ottesen

Sandia National Laboratories, Livermore, California 94550

ABSTRACT

External reflectance infrared spectroscopy has been used to study the formation of oxide films on chromium and iron alloys. Experimental data have been acquired with an FTIR spectrometer using a polarized beam at high angles of incidence to the surface normal. Theoretical calculations have been made for these systems and are compared with the experimental results. Particular attention is given to the quantitative calculation of film thickness. Complications which arise from distortions in band shape, frequency shifts, the appearance of additional reflectance minima, and beam divergence and state of polarization are discussed in detail.

This paper presents an experimental and theoretical study on the applicability of Fourier transform infrared (FTIR) reflectance spectroscopy for the study of oxide films formed on binary iron-chromium alloys. A thorough understanding of these results is a vital step leading to the study of more complex ferrous alloys, such as the stainless steels. The quantitative study of metal alloy oxidation and corrosion using this technique requires a detailed understanding of the physical processes governing the optical properties of such layered systems. We have also sought to determine the effect of nonidealities, such as the roughness of films and substrate, and variations in experimental parameters, such as the angle of incidence, beam divergence, and state of polarization.

Infrared spectroscopy has played an increasingly important role over the past few years in the chemical characterization of surfaces. In particular, external reflection spectroscopy at large angles of incidence has been of special value in examining thin, dielectric films on metallic substrates. The usefulness of this technique was first noted by Berreman (1) and later popularized by Greenler under the name "reflection-absorption spectroscopy" (2-4).

Reflection-absorption spectroscopy has much in common with ellipsometry, another surface-sensitive optical technique. While both approaches utilize linearly polarized light, visible wavelength ellipsometry has generally been acknowledged to be the more sensitive technique to small changes in surface coverage. This is due to the clearly observed changes in phase angle of light reflected from a substrate covered by a dielectric film only a few angstroms thick. This advantage, however, has been offset somewhat by recent developments in double-modulation FTIR reflectance spectroscopy (5).

The outstanding advantage of reflection-absorption spectroscopy lies in the positive identification of chemical species in surface films through the spectral structure in the observed reflectance. In general, ellipsometry suffers from the lack of spectral data in single wavelength measurements, with the consequent assumption of surface species and their optical constants. Even scanning ellipsometric measurements in the visible region can be relatively featureless, resulting in unavoidable ambiguities in the determination of surface species (6).

Reflection-absorption spectroscopy has been successful in a large number of recent qualitative investigations. Interest has centered primarily on the characterization of chemisorbed gases (5, 7) and thin layers of organic compounds deposited on metals (7-13). Reference (7) is a particularly useful review article of results up to 1976.

Investigations of inorganic thin films on metallic substrates have also been numerous (1, 4, 14-24). These results are qualitatively quite different from the studies of chemisorption and thin organic films. The interpretation of the resulting reflectance spectra for these systems is complicated by distorted band shapes and frequency shifts for thin films when compared to absorption spectra of the pure, bulk material. This behavior is generally caused by the large values of refractive index and absorption coefficient associated with the absorbing film and the metallic substrate and the complex interaction of these optical properties with the electric field of the incident infrared beam. In addition to our own experimental work on metal oxides, we will draw on earlier spectroscopic studies of the high temperature oxidation of iron (14, 18) and chromium (24).

Theoretical

We will adopt the nomenclature of Heavens (25) in our treatment of the interaction of light with a thin film on a bulk substrate. This is shown for an n-layer film in Fig. 1. Here n_m and k_m are the refractive index and absorption coefficient, respectively, d_m is the thickness of the layer, and Φ_0 is the angle of incidence, while Φ_m ($m > 0$) is the angle of refraction within a layer, m. For absorbing media, we also note that the refractive index and angle of refraction are in general complex. In this case, the so-called complex refractive index is defined as

$$\hat{n}_m = n_m - ik_m \qquad [1]$$

The amplitude of the electric field both incident and reflected from this system of layers can be expressed by solving Maxwell's equations in terms of these quantities. Using the boundary conditions that the tangential components of both the electric and magnetic vectors be continuous at each layer interface, we arrive at the expression shown in Eq. [2] and [3] for the ratio of the electric field amplitudes in the plane where layer m is in contact with layer $m + 1$

$$E^-_{mp}/E^+_{mp} = [(\hat{n}_m \cos \Phi_{m+1}) - (\hat{n}_{m+1} \cos \Phi_m)]/[(\hat{n}_m \cos \Phi_{m+1}) + (\hat{n}_{m+1} \cos \Phi_m)] \qquad [2]$$

$$E^-_{ms}/E^+_{ms} = [(\hat{n}_m \cos \Phi_m) - (\hat{n}_{m+1} \cos \Phi_{m+1})]/[(\hat{n}_m \cos \Phi_m) + (\hat{n}_{m+1} \cos \Phi_{m+1})] \qquad [3]$$

These ratios are more commonly known as the Fresnel reflection coefficients, r_{mp} and r_{ms}, where P and S refer to the polarization of the light. The change in phase of the